
On the Vortex Wake of an Animal Flying in a Confined Volume

Jeremy M. V. Rayner and Adrian L. R. Thomas

Phil. Trans. R. Soc. Lond. B 1991 **334**, 107-117
doi: 10.1098/rstb.1991.0100

Email alerting service

Receive free email alerts when new articles cite this article - sign up in the box at the top right-hand corner of the article or click [here](#)

To subscribe to *Phil. Trans. R. Soc. Lond. B* go to: <http://rstb.royalsocietypublishing.org/subscriptions>

On the vortex wake of an animal flying in a confined volume

JEREMY M. V. RAYNER AND ADRIAN L. R. THOMAS†

Department of Zoology, University of Bristol, Woodland Road, Bristol BS8 1UG, U.K.

SUMMARY

When an animal flies near a boundary, the airflows it generates interact with that boundary. These interactions may have a significant effect on flight performance, as measured by quantities such as the energy rate to sustain flight, or the circulation of the vortices bound on the wing or shed in the wake (or, equivalently, by the lift and induced drag coefficients). The problem of hovering and slow flight within a confined volume is considered by a theoretical model based on helicopter practice, and by flow visualization experiments. The wake takes the form of a strong recirculating flow within the volume, and because of this recirculation the boundaries appear to cause a large reduction in the induced power required for sustained flight, even when their distance from the animal is several times greater than the wingspan. The correction factor relative to ideal momentum jet theory is greater than for the hovering ground effect, forward flight ground effect, or wind tunnel wall interference problems at comparable distances. The flow pattern that develops in the presence of floor and wall interactions in hovering or slow flight includes a large-diameter vortex ring trapped underneath the animal; this vortex ring is conjectured to be analogous to that below a helicopter in slow descending flight in the 'vortex ring state'. Performance measurements for animals in hovering flight within a confined volume may underestimate power for free hovering by a significant margin. Comparable boundary effects may also be important in confined forward flight. Because of speed-related changes in the wake, and the rise in induced power at lower speeds, the appropriate correction to total mechanical power is dependent on air speed, becoming progressively greater as speed reduces. Some wind tunnel measurements of total metabolic power have produced the apparently anomalous result that power is independent of flight speed within measurement error. These observations may be explained – at least in part – by boundary effects caused by interaction between the wake and the walls of the wind tunnel.

1. INTRODUCTION

In this paper we consider the flow patterns generated by a hovering or slow flying animal within a confined volume. By flow visualization experiments and theoretical predictions we illustrate the mechanisms by which the boundaries of the space in which the animal flies interfere with the airflows it generates, and thereby affect its flight performance. We are drawn to this problem as a means of calibrating experimental results, and do not claim it to be a particularly realistic biological situation. The imagination must be stretched to find examples where animals habitually sustain flight within confining boundaries which affect their flight in the ways we discuss here: the gleaning flight of certain small insectivorous bats within foliage is one of the few examples which come to mind. However, it is common for the hovering flight performance of insects and small vertebrates to be determined experimentally as the animals sustain flight within a confined volume. This approach has obvious experimental advantages as – if the volume is airtight – changes in gas concen-

tration can be measured to enable metabolic power to be computed. Little consideration has been given to the possible aerodynamic consequences of this protocol, in particular those caused by proximity to boundaries, and experimenters have implicitly relied on the familiar, but untested, 'rule of thumb' that boundaries more distant from the animal's centre than two or three times the wing semi-span have no material effect on performance. This is based on experience with fixed wing models in wind tunnels; we question its applicability to hovering flight, and tentatively also to forward flapping flight.

We are concerned primarily with flight within a confining volume with boundaries surrounding the animal on all sides (we model this volume by a cube with impermeable boundaries). The basic concept of the model can also be applied with little modification to flight in the presence of less confining boundaries, and in particular to flight in a wind tunnel, or (in still air) in a flight cage, in which four faces (two sides, floor and roof) are bounded, but two sides are open. The derivation of wind tunnel interference corrections for a lifting wing is a classical problem of slow speed aerodynamics; the related problem of flight within ground effect is also familiar, although in fact it is

† Present address: Department of Zoology, University of Cambridge, Downing Street, Cambridge CB2 3EJ, U.K.

frequently misapplied, and has more obvious applications to animal flight.

2. THEORETICAL ANALYSIS

(a) *Boundary interference over the ground*

We seek a conceptually straightforward theoretical model describing the change in performance of a flying animal within a confined volume. The primary intention is to explore the accuracy of performance measurements made in such circumstances, and to derive a method of assessing the dimensions of flight cages for which boundary interactions can safely be ignored.

The force generated by a flying animal is the reaction of momentum transported away from the animal in the form of a vortex wake, which is generated by bound vortices on the animal's wings (Rayner 1988). The primary mechanism by which confining surfaces influence performance is the distortion of the vortex wake by those surfaces. Interaction of vortices with a surface are usually modelled theoretically by developing a system of images so that there is no flow perpendicular to the surfaces. For a plane surface the image vortices are simply the reflections of all vortices within the flow (including any other image vortices). This method is conventionally used to estimate the effect of wall interactions for aircraft wings or wing models within a wind tunnel (see, for example, Milne-Thompson 1958; Pope & Harper 1966), and to quantify forward flight in ground effect for aircraft (see, for example, Reid 1932; Küchemann 1978; Laitone 1989; Rayner 1991); the resulting numerical estimates of the effect of the ground on induced drag have been applied also to birds and bats (see, for example, Blake 1983; Hainsworth 1988; Kistiyakovskii 1967; Aldridge 1988; Withers & Timko 1977; Rayner 1991). In these cases, the parent vortex system within the flow field comprises the bound vortex on the wing, and the trailing vortices behind the wingtips. The image method is conceptually valuable in indicating how proximity to the ground affects the flow, and it gives tolerably accurate measures of performance as long as the wing is not very close to the ground. None the less, it is not fully realistic physically: there are changes in the boundary layer and the pressure distribution on the wing when close to the surface (Küchemann 1978), and the trailing vortex pair can induce boundary layer separation on the ground plane: secondary and tertiary vortices develop in the ground boundary layer and are drawn off to amalgamate with, or interfere with, the wingtip vortices (Harvey & Perry 1971; Doligalski & Walker 1984; Ersoy & Walker 1985).

The problems of forward flight in a wind tunnel and in ground effect differ from that of hovering flight within a confined volume in that the wake vortices always lie more or less parallel to the bounding surfaces. An indication of a suitable approach to the hovering problem can be drawn from the hovering ground effect problem. The usual model for the wake of a hovering animal, a propeller or helicopter is the

Rankine–Froude momentum jet: the classical theory of the ideal momentum jet models the animal's wings, the propeller blades or the helicopter rotor as an actuator disc which imparts a pressure difference to air passing through it (see, for example, Glauert 1947; Lighthill 1979; Rayner 1979*a*; Ellington 1984; Spedding 1991). The wing disc is usually modelled as circular, and can be envisaged as the source of a circular vortex tube which forms the boundary of the momentum jet beneath the disc. This vortex tube induces airflows within the wake which transport momentum downwards, and the reaction of this momentum flux is the lifting force which balances weight; as a result of momentum conservation within the wake the tube contracts to half the diameter of the wing disc in the far field below the disc.

When birds and helicopters (and indeed some fish, (Blake 1979)) hover over a surface, the wake forms a roughly cylindrical vertical tube; the tube approaches normal to the ground plane, with which it interacts by spreading out sideways over the surface (Betz 1937). This distortion of the momentum jet reduces the magnitude of downwards airflow required for sustained hovering, and therefore the induced power is lower than that for flight in the absence of the ground plane. Two theoretical approaches to this problem have been advanced, both of which model the hovering wake as an axisymmetric circular vortex tube. Knight & Hefner (1941) modelled the wake boundary as a cylindrical tube, and estimated downwash on the wing disc from the velocities induced by two segments of tube: that between the helicopter and the ground, and its mirror image below the ground plane. Lighthill (1979) gave a more complete and mathematically robust model of the hovering ground effect flow in two dimensions, estimating in particular the shape of the free streamline (or equivalently of the vortex tube) bounding the momentum jet. Knight & Hefner's (1941) model has the limitation that it fails to account for contraction of the momentum jet below the wing disc (Lighthill 1979). None the less, at moderate and large distances above a surface (height/wing disc radius > 1), both this and Lighthill's model agree reasonably well with each other and with empirical measurements of helicopter performance (see, for example, Zbrozek 1947), at least when allowance is made for tip losses at the wing disc. Lighthill formulates the predictions of his model for hovering with a two-dimensional momentum jet in ground effect as a correction factor to the ideal theory for free hovering; he argues that these factors will also be valid as corrections for more realistic models of hovering in which tip losses and intermittency of force generation at the wing disc are accounted. Such models for animal hovering have been developed by Rayner (1979*a*) and Ellington (1984) by visualizing the intermittent wake as stacked vortex rings; in these models performance can also be expressed in the form of correction coefficients to ideal momentum jet theory. It seems reasonable to accept Lighthill's proposition that ground effect (or confining volume) correction coefficients relative to the ideal momentum jet could be applied equally to these models.

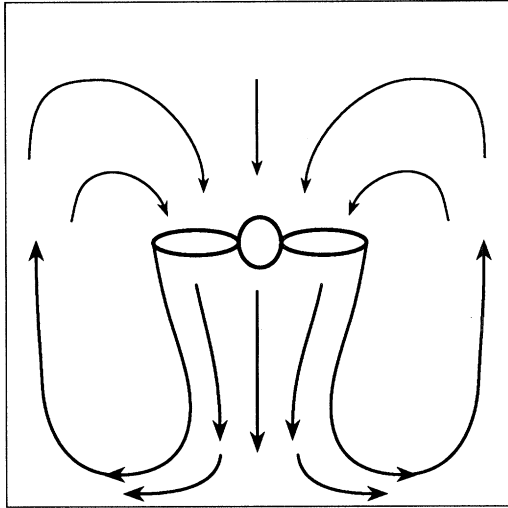


Figure 1. Conceptual model of the airflow created by an animal hovering within a confined volume, modelled on the basis of the ideal momentum jet theory and Lighthill's (1979) two-dimensional hovering momentum jet ground effect theory. The momentum jet generated at the wing disc (heavy line) spreads sideways at the ground plane, and up along the sides of the volume, before being drawn in towards the wing disc. This has the effect of producing a recirculation within the lower half of the volume, below and outside the animal.

(b) *Flight in a confined volume*

Within a confined space, the flow is inevitably more complex than with the ground plane alone, as the wake can interact with the side walls and the roof as well as with the floor. (The term 'confined' is used here in the sense that air flow is restricted and does not influence, or is not influenced by, air outside the volume; it does not necessarily imply that flight is within an airtight box. It should be noted, however, that if for practical or physiological reasons observations are made within an airtight volume, then fluid mechanical complications of the type discussed in this paper will inevitably be significant.) Despite the similarities between the problems of flight within a volume and in ground effect, this situation does not appear to have been treated theoretically hitherto.

The airflow generated by an animal hovering within a rectangular volume can be visualized conceptually (figure 1). The momentum jet below the animal interacts with the ground and spreads sideways, much as it does over the ground alone (see, for example, Lighthill 1979). The flow above the floor is radially outwards, and will in time interact with the side walls, which will deflect it upwards. Then the flow will be directed inwards by the roof and by the suction on the actuator disc, and will be forced to recirculate down towards the animal, and again through the wing disc. In the steady state, when the animal has had a long period in which to affect the flow, the bulk of the fluid within the volume will have been influenced by the beating wings; energy added to the flow at the wing disc in the form of vortices and vortex-induced downwash is then dissipated by friction as the induced flows pass floor, walls and roof. The main character-

istics of the flow according to this argument will be a momentum jet below the animal (which may be intermittent because of wing flapping), and a large scale recirculation within the volume. Vorticity generated at the wing disc cannot disappear by reaction with the floor as the axes of the vortices generated are perpendicular to the floor; this vorticity must accumulate as a vortex loop lying parallel to the plane of, but probably being much larger than, the animal. The situation may therefore be very different from that in free hovering, where vorticity travels away indefinitely below the animal, and air at some distance laterally from the animal is largely unaffected by the wing disc and its wake. It would seem from this argument that the effect of the recirculation will be to add a downwards flow to the velocities induced at the wing disc. However, this is not in fact the case, as the greatest effect on the flow is that of the ground plane, and distortion of the vortices bounding the momentum jet reduces the induced downwash required to generate sufficient lift to support weight; the total flow over the wing disc (and hence the induced power) will be lower than in unconfined hovering; this result will be derived formally below.

The model presented in this paper is based on the inviscid flow generated by a system of concentrated vortices, and which is otherwise irrotational. It must be set against the background of the argument above in which viscous (frictional) forces limit the flow in its steady state: it would be unreasonable to rely too strongly on an inviscid, irrotational model of what is necessarily a highly complex, viscous-dominated flow. However, an inviscid model is both computationally and conceptually straightforward, and indicates the trend of the effect of the boundaries, just as comparable inviscid models give reasonably realistic estimates of the performance costs, if not of the actual flows developed, for the forward flight and hovering ground effect problems (see above).

(c) *Formulation of the model*

The model of hovering within a confined volume can be divided into two phases.

I. The animal will appear to be hovering (hovering is defined for the purposes of this paper as flying so that the centre of gravity is stationary relative to the ground) in an upwash of magnitude w . This upwash affects the induced downwash u_i across the wing disc and the pressure distribution (p above and $p + \Delta p$ below) around the wing disc, and reduces the induced power P_1 required compared to free hovering (in an infinite volume) with no external air movements. How do these quantities depend on w ?

II. The upwash w is generated by the airflows in the animal's wake as they interact with the boundaries. By analogy with the ground effect problem it may be modelled as the air velocity induced by the image vortices of the boundary of the momentum jet. In steady hovering the lift generated by the wing disc in the presence of w must balance the weight. This force equilibrium condition can be formulated as a constraint relating w to the self-induced downwash u_i and

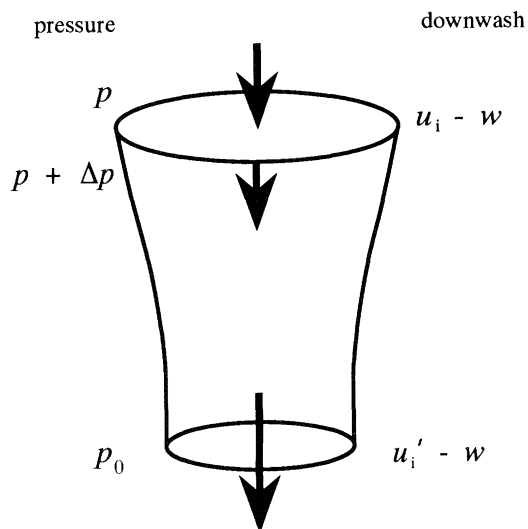


Figure 2. Notation for the momentum jet theory in the presence of an externally applied upwash w . See text for further details.

to the geometry of the wing disc and the bounding volume, from which the strength of the actuator disc is determined.

(i) *Phase I: momentum jet theory in an imposed upwash*

Provided the upwash w is not too large, phase I of the problem can be formulated as a simple modification to the ideal hovering momentum jet theory. Relative to the animal, the airflows applying to hovering in an externally applied upwash are the same as those in a slow vertical descent, which is a familiar (if formally unsolved) problem for helicopters; it is similar also to the axial flow through a propeller in reverse thrust (Glauert 1947). The following argument is based on the theory given for slow vertical descending flight of a helicopter by Johnson (1980), in notation consistent with that used by Rayner (1979*a*). The theory for the ideal hovering momentum jet can be reclaimed from the following by substituting $w = 0$.

The basic concepts of momentum jet theory are illustrated in figure 2. Fluid far from the disc is at ambient pressure p_0 . The wing disc adds energy to the flow in the form of a negative pressure difference Δp , which is identical to the disc loading Mg/A (where M is the animal's mass, g is the acceleration due to gravity, and A is the area of the wing disc, which is equivalent to a circle of diameter equal to the wingspan b). Air passing through the wing disc is accelerated downwards by the disc to the speed u_i , known as the induced downwash, so the airflow through the disc has downwards velocity $u_i - w$. In the far wake below the wing disc pressure has returned to ambient, and has downwards velocity $u_i' - w$. Within the jet both above and below the wing disc mass, momentum and energy are conserved. The mass flux through the wing disc is

$$\mu = \rho A(u_i - w). \quad (1)$$

Momentum is added to the flow at rate

$$T = \mu(u_i' - w) + \mu w = \mu u_i', \quad (2)$$

such that the force T generated at the wing disc balances the weight Mg in steady hovering. The induced power P_i is the rate at which energy is added to the flow at the wing disc, and therefore

$$P_i = T(u_i - w); \quad (3)$$

drag forces from the upwash w as it passes the animal's body and wings are considered negligible. Because energy is conserved in the wake, this quantity must also equal the rate of increase of kinetic energy between the far wake above and below the wing disc, so that

$$T(u_i - w) = \frac{1}{2}\mu(u_i' - w)^2 - \frac{1}{2}\mu w^2 = \frac{1}{2}\mu u_i'(u_i' - 2w). \quad (4)$$

By eliminating T/μ from equations (2) and (4), we find $u_i' = 2u_i$, and so, from conservation of mass within the far wake below the wing disc, conclude that the wake cross-sectional area must contract by the factor $(u_i - w)/(2u_i - w)$; when $w = 0$ the wake contracts by $\frac{1}{2}$, the familiar result for the ideal momentum jet, but as w increases the wake contracts further.

The above equations can be solved to yield the induced downwash u_i at the wing disc as

$$u_i = \frac{1}{2}w + \frac{1}{2}\sqrt{(w^2 + 4u_0^2)}, \quad (5)$$

where u_0 is the induced velocity for the ideal free momentum jet without upwash ($w = 0$), which is given by $\sqrt{(Mg/2\rho A)}$. The positive branch of the square root is chosen to ensure consistency when $w = 0$; for large values of w , beyond those considered here, the negative branch may be required, but the formal solution then ceases to be valid. The induced power is obtained by substitution in equation (3) as

$$P_i = P_{i0}\{- (w/2u_0) + \sqrt{[(w^2/4u_0^2) + 1]}\}, \quad (6)$$

where P_{i0} is the induced power for the free momentum jet, namely Mgu_0 . The induced power factor P_i/P_{i0} measures the effect of the upwash, and following Lighthill (1979) is identified by C_p , the induced power factor. It takes the value 1 for the ideal momentum jet, and lower values when ground effect reduces the energy rate required to hover.

It must be emphasized that this theory is valid only for small values of w , and even in this situation it suffers from a number of limitations (see below). For large w , the total flow through the wing disc becomes small, or can reverse direction. This is associated with other changes in the flow pattern close to the wing disc which can have a material effect on performance and on the airflow within the volume.

(ii) *Phase II: determination of the upwash*

In deriving the momentum jet solution in phase I the upwash w was unknown, but was taken to be positive and small compared to u_i . The momentum jet generated by the animal can be modelled as a vortex tube with a vertical axis lying below the animal, and with all vorticity azimuthal and confined to horizontal circular loops. The circulation per unit length κ of this tube is identical to u_i' (Rayner 1979*a*). This vortex structure induces a vertical downwash across the wing disc and within the tube. In the isolated ideal momentum jet, the tube contracts below the wing disc, but as the tube is semi-infinite in length the induced

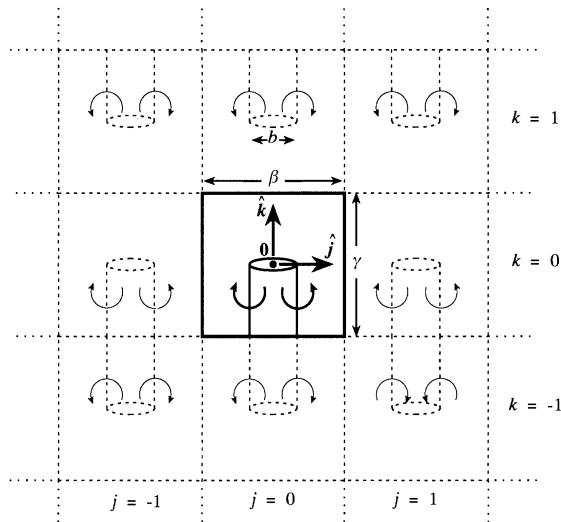


Figure 3. The image system for the momentum jet of diameter b within a confined rectangular volume (height γ , widths α and β). The parent jet and the box enclosing it are shown as solid lines. The images (dashed) repeat also along the \hat{x} axis, normal to the paper. Alternate images in the floor and roof of the volume have opposite circulation; images in the walls have circulation with the same sense as the momentum jet.

velocity at the wing disc is uniform across the disc (see below).

For hovering within a confined volume, w is calculated as the velocity induced by a system of image vortices comprising the reflections of the parent vortex tube bounding the momentum jet in the walls, floor and roof of the confining volume. We assume this volume to be rectangular, with all six faces formed by solid planar surfaces. (The alternative of a cylindrical volume has the advantage of symmetry, but is less tractable mathematically.) The image system is therefore a repeating pattern extending to $\pm\infty$ along all three axes, with spatial period equal to the appropriate side length of the box, and with alternate vortices reflected in the planes forming the floor and roof having circulation of opposite sense (figure 3). We model the image vortices as cylindrical segments, thus ignoring the effect of contraction of the wake. This assumption is necessary as the shape of the boundary of the 3-dimensional ideal momentum jet is unknown. It can be justified by the fact that it will have a relatively small effect on the velocity induced by the image; moreover, the wake expands close to the floor of the volume, and will not contract as much as the ideal jet. Neglect of the contraction of the parent momentum jet is not justified, as this has a material effect on the induced downwash (Lighthill 1979); this assumption is, however, not necessary, as u_i is computed exactly from equation (5).

The induced upwash w is proportional to the circulation per unit length within the vortex tube, and depends otherwise on the geometry of the system, namely the wingspan b and the dimensions α , β and γ of the bounding box (figure 3); w may be written

$$w = Q(b, \alpha, \beta, \gamma) \kappa, \quad (7)$$

where Q is a quantity to be determined which depends solely on the geometry, and which is here termed the interference coefficient.

As $\kappa = u'_i = 2u_i$, equations (5) and (7) may be combined to form an identity which should be interpreted as the equivalent of the force balance across the wing disc; w must satisfy

$$w = Q[w + \sqrt{(w^2 + 4u_0^2)}], \quad (8)$$

from which w may be determined as

$$w = 2u_0 Q / \sqrt{(1 - 2Q)}. \quad (9)$$

Finally, from equation (6), the induced power factor may be obtained in terms of Q as

$$C_p = \sqrt{(1 - 2Q)}. \quad (10)$$

This solution is valid for $0 \leq Q < \frac{1}{2}$. The limit $Q = 0$ corresponds to the case of no induced upwash w , or no image system. In the presence of the image system, $Q > 0$, and induced power is reduced. The other bound $Q = \frac{1}{2}$ corresponds to the situation in which the upwash w induced on the wing disc by the images equals the downwash induced by the momentum jet. This is a well known complication of the reverse thrust propeller and the helicopter descending flight problems (see below); beyond this constraint the flow through the wing disc is vertically upwards, the far field outflow in the wake is above the animal, and it is physically unrealistic to model this situation by the vortex tube and image system. However, this condition arises only when the box is not much larger than the wingspan ($\beta \lesssim 1.5b$) and the image vortices are relatively close to the wing disc. We trust that investigators of hovering flight have not expected animals to perform naturally in these circumstances, but at the present we are unable to predict the likely flow patterns and changes to performance. Our analysis indicates they are likely to be considerable!

The interference coefficient Q is determined by computing w/u_0 for the image system of the momentum jet. Each image consists of a vortex tube of circulation per unit length $\kappa = \pm u'_i$, diameter equal to the wingspan, b , and height, $h = \pm \frac{1}{2}\gamma$. Let $\kappa \mathbf{U}(\mathbf{x}; \mathbf{t}, h)$ be the downwards velocity induced at \mathbf{x} by such a tube, whose centre (the image of the centre of the wing disc) is \mathbf{t} . For the ideal momentum jet we have $\mathbf{U}(\mathbf{x}; \mathbf{0}, \infty) = \frac{1}{2}$ for all \mathbf{x} on the wing disc ($\mathbf{x} \cdot \hat{z} = 0$, $|\mathbf{x}| < \frac{1}{2}b$). The interference coefficient Q for the upwash w at the centre of the wing disc $\mathbf{x} = \mathbf{0}$ can be determined from

$$Q = - \sum_{\substack{i, j, k = -\infty \\ i=j=k \neq 0}}^{\infty} (-)^k \mathbf{U}(\mathbf{0}; \mathbf{t}_{ijk}, \frac{1}{2}(-)^k \gamma) \cdot \hat{z}, \quad (11)$$

where \hat{z} is the vertical unit vector; i, j, k denote summation over the \hat{x} , \hat{y} and \hat{z} axes, respectively, and

$$\mathbf{t}_{ijk} = (i\alpha, j\beta, k\gamma). \quad (12)$$

Strictly the image elements should account for contraction of the momentum jet, and should be circular, but not cylindrical. The degree of contraction of the three-dimensional jet is unknown, but computations with images with a linear taper to half the disc diameter show appreciable differences ($> 10\%$ in $|Q|$)

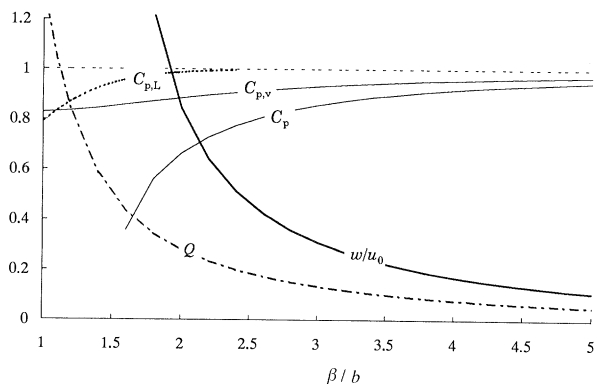


Figure 4. Effect of box size on performance for an animal hovering at the centre of a cubic volume. Q , interference coefficient; w/u_0 upwash induced by the image system; C_p , induced power factor. Also shows induced power factor for hovering between horizontal planes (spacing β) ($C_{p,v}$), with the vertical image system only, and for hovering in ground effect (height $\frac{1}{2}\beta$) ($C_{p,L}$), calculated from equations (18) and (22) of the two-dimensional model of Lighthill (1979). Calculations were performed on a Tandon PCA-486s1 microcomputer, with programs in Microsoft Basic PDS v. 7.1 written by J. M. V. R.

from the results given below only for very small volumes ($\beta \lesssim 1.25b$); accordingly the simpler cylindrical image system is used here.

Knight & Hefner (1937) have shown that $\mathbf{U}/U \cdot \hat{\mathbf{z}}$ may be calculated as $1/4\pi$ times the difference in the solid angle subtended at $\mathbf{0}$ by the two ends of the tube. However, it proves more convenient to compute \mathbf{U} from the integral of the stack of vortex rings forming each vortex tube. The formulation of the integrals and summation in terms of the induced velocity of an isolated circular vortex ring (see, for example, Lamb 1932; Rayner 1979*a*) is straightforward, and the details are not repeated here.

Results of the image system computation for a cubic volume $\alpha = \beta = \gamma$ are shown in figure 4. It is seen that, for all image configurations, $w > 0$; this confirms the claim made above that the recirculating flow within the volume reduces the total downwash. The effect of the upwash induced at the wing disc by the image system can be considerable. With $\beta/b = 2$ we find $w/u_0 = 0.844$, $Q = 0.280$, and $C_p = 0.663$, a reduction of approximately $\frac{1}{3}$ in induced power. Thus, it is foolish to image that the performance of an animal flying within a confined volume is unaffected by its boundaries. Even with a much larger volume $\beta/b = 4$ the predicted effect on induced power is still appreciable: $w/u_0 = 0.170$, $Q = 0.078$, and $C_p = 0.919$.

For comparison, figure 4 also shows the induced power factors computed for two comparable situations, namely for the two-dimensional hovering case ($C_{p,L}$) modelled formally by Lighthill (1979), and the three-dimensional case for hovering between horizontal planes ($C_{p,v}$), derived from the model above with $\alpha = \beta = \infty$ (and hence no i and j summations). An appreciable reduction in induced power is traceable to the presence of the side walls, which, as argued above, encourage a vertically upwards recirculation in the region outside the momentum jet. A crude indication

of the structure of this flow can be derived by computing the induced velocity $\mathbf{U}(\mathbf{x}; t, h)$ for \mathbf{x} within the cubic region $-\frac{1}{2}\beta \leq x, y, z \leq \frac{1}{2}\beta$, and adding the velocity $\mathbf{U}(\mathbf{x}; \mathbf{0}, \frac{1}{2}\gamma)$ induced by the parent momentum jet, assumed for this part of the calculation to be formed by a segment of cylindrical vortex tube. The vertical component of the induced velocity is computed from equation (11), including the summation term $i = j = k = 0$ for the parent jet; the horizontal components are derived from the similar equations for the $\hat{\mathbf{y}}$ and $\hat{\mathbf{z}}$ axes. The resulting flow patterns are shown in figure 5. For an infinite volume, $\beta = \infty$ and the jet extends to $-\infty$; the flow has circular symmetry, and the predominant motion is vertically downwards within the tube (figure 5*a*). This is not a serious limitation as downwash on the wing disc is relevant to performance in the interference problem, and this is correctly estimated. Downwash across the wing disc is constant (and equal to $\frac{1}{2}\kappa$). There is a weak inflow as fluid is drawn towards the plane of the wing disc. Strictly, all downflow should be confined to the interior of the tube; this model predicts a downflow outside the tube also because contraction of the free streamline forming the boundary of the tube is neglected. When the flow is bounded (figure 5*b, c*) the pattern is significantly altered: flow is no longer uniform within the momentum jet, particularly as it approaches the ground plane; a strong outflow develops on the ground plane, as well as an intense recirculation that is generally confined to the region $0.75b < |\mathbf{x}| < 1.25b$, except where the boundary is closer than $1.25b$; in this case a strong upflow develops close to the walls and corners of the box (figure 5*c*). The inflow is slightly above the plane of the wing disc, and when the animal is hovering at the centre of the box the roof of the bounding volume has little apparent influence on the flow; however, images in that roof do have a material effect on the lateral flow towards the wing disc. It must be noted that the recirculation within the volume is modelled as irrotational (other than in the wall and floor boundary layers). In practice this cannot be valid, for the model provides no sink for vorticity being convected towards the floor. Lighthill (1979) has described how this vorticity will spread over the ground plane. Within the confined volume it will become trapped within the region of recirculation, which, as explained above, may be expected to take on the characteristics of a circular vortex ring, and in turn to influence flow over the wing disc. For this reason, our approximation of C_p is likely to be an overestimate, and the effect of the bounding volume to be to reduce C_p compared with the values we predict in figure 4. A physical analogy to this process – the vortex ring state of a helicopter rotor or propeller – is discussed below.

(d) Limitations of the model

For several reasons we are reluctant to suggest that the simple theory presented here is adequate as the basis of a correction factor which might be applied to experimental performance (e.g. metabolic power) measurements. But as an indication of the potential influence of the boundaries, and thereby an indication

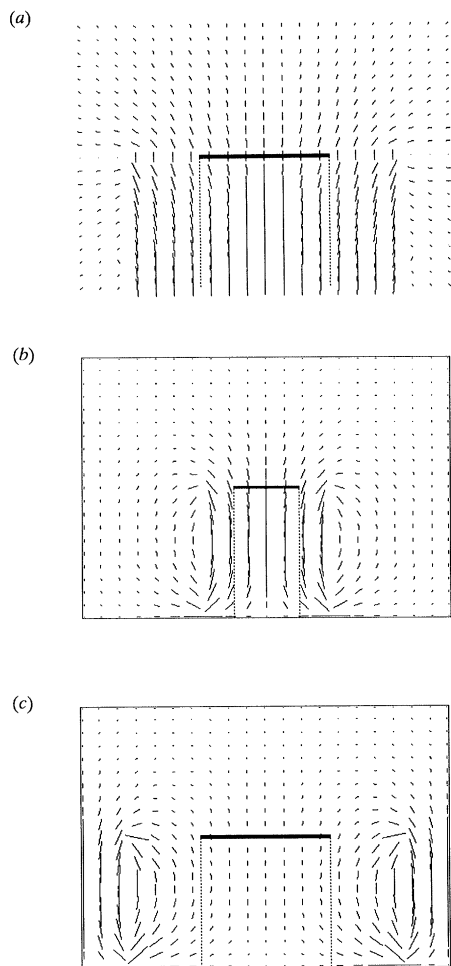


Figure 5. Flow patterns developed by the momentum jet and its image system within a cubic volume. (a) Flow without boundaries: the flow is close to that from an ideal semi-infinite momentum jet, except that the degree of contraction of the jet is underestimated, and therefore a downwash is induced outside the disc. (b) Flow within a relatively large volume $\beta/b = 4$. A strong outflow has developed on the ground plane, with a diffuse recirculation in the region $0.75b < |x| < 1.25b$. (c) $\beta/b = 2$. The flow is similar to that in (b), except that the recirculation is confined by the side walls and is markedly more intense. In all figures the solid horizontal bar marks the position and dimensions of the wing disc, and the dotted lines the boundary of the momentum jet (assumed circular). Flow lines are drawn proportional to the local flow velocity computed at each point, but the three drawings are to different scales. In (b) and (c) the section drawn is the diagonal of the cube, from $x = y = -(1/\sqrt{2})\beta$ to $x = y = +(1/\sqrt{2})\beta$.

of the need for caution in interpreting measured flight performance, it has considerable value. There are several reasons for doubting the precise numerical predictions of the theory.

1. As explained above, friction on the walls has a significant limiting effect on the flow in its long-term steady state. This force is neglected in an inviscid, locally irrotational model. Friction may slow the spreading of rings on the floor of the volume, thereby reducing upwash, and increasing C_p . However, drag of the airflow past the animal's body would in turn reduce C_p . Further, the vortex boundary of the

momentum jet spreading over the ground plane may cause the ground boundary layer to separate, particularly as it approaches the edges or corners, and the boundary layer may also be unstable at the mid-point of the walls where it is moving most rapidly; the development of separation or of interacting vortex flows would presumably depend on Reynolds' number, that is on the size and mass of the animal (as evinced in the size and strength of the wake vortices), and the size of the confining box. This process is discussed for an isolated vortex ring by Walker *et al.* (1987).

2. Contraction of the wake (momentum jet) in the image vortices is neglected, although contraction of the momentum jet of the parent wake has a material effect on the airflow around the wing disc (Lighthill 1979). We do not believe that neglect of image contraction is of great significance because the image is spatially distant from the wing disc.

3. The actuator disc-momentum jet model is a good 'first approximation' to animal hovering (as indeed it is also for the helicopter), but itself requires amendment in various ways to be realistic. Allowance may be needed for intermittency of force generation by the beating wings, for tip losses caused by roll-up of the vortex sheets shed by each wing, for angular velocities within the plane of the wing disc (which are of constant sense in the helicopter case, but which alternate in a hovering animal), and for the fact that the beating wings may not traverse the entire wing disc. We follow Lighthill (1979) in claiming that corrections derived here for the presence of the bounding planes with a steady momentum jet are broadly similar to those that would be appropriate to modify a realistic model of induced power in animal hovering.

4. In a hovering animal, the flapping wings rarely remain planar on the wing disc, but at some points of the wing stroke will be closer to one or other of the boundaries. This effect will be most significant in particularly small volumes.

5. There are well known complications of momentum jet theory when applied to descending vertical flight (Johnson 1980; Shi-Cun 1990). Similar problems apply to the propeller in reverse thrust (Glauert 1947). The difficulties arise because far above the wing disc the induced upwash caused by the images exceeds the downwash caused by the parent wing disc. Thus, at high descent rates, or equivalently with a high externally imposed upwash, the nett airflow above the wing disc is upwards and away from the disc. The conditions of conservation of mass, momentum and energy in the forms given in equations (1)–(4) are therefore invalid. In a helicopter or propeller this situation is known as the vortex ring state: the vortices shed from the ends of the blades, and which normally form the boundary of the momentum jet, are trapped close below the wing disc, where they accumulate to form a large, and unstable, vortex ring. This ring introduces significant problems of control and stability, partly because it has an immediate effect on the thrust required to sustain steady, level hovering, and partly because of its tendency to shift vertically.

None of these potential limitations are likely to alter our conclusion that the boundaries to the flight space

have a much greater effect on performance than is usually supposed. Indeed, the effect of including most of these potential amendments to the model would be further to reduce induced power. Of the problems listed, (5) seems to be the most serious. We can only conjecture that comparable flow patterns develop in the vicinity of an animal hovering in a confined space. It seems reasonable to suppose that such patterns, no doubt complicated by the effect of the flapping wings, would apply in the case of an animal in descending hovering flight, or in hovering within a confined volume, just as they do for the helicopter. We present some limited experimental evidence below. If this is the case, then – as for the helicopter – there is currently no adequate theory predicting performance applicable to this situation. Empirical observations for helicopters in descending flight show that when $|w| < |u_0|$, that is at low descent rates (or in our situation with reasonably distant boundaries $\beta/b > 2$), the momentum jet model with $w > 0$ (equation (10)) gives reasonably accurate estimates of induced downwash and induced power, when allowance is made for tip losses (Johnson 1980), despite the formal breakdown of the conservation equations. However, the trapped vortex ring is still likely to develop in this case unless w is very small. At higher values of w the state of the airflow around the wing disc changes dramatically, and shows large scale, unstable turbulent vortex structures. According to the model above this would be likely to occur for box: wingspan ratios $\beta:b$ less than approximately 1.75 (figure 4; C_p falls towards 0).

(e) *Forward flight*

In fast forward flight the corrections appropriate for flight with a fixed wing within a tunnel with open ends (such as a wind tunnel) are relatively modest. For a bird flying at the centre of a square tunnel of cross section width equal to twice the wingspan, the reduction in induced drag or induced power is estimated as 23.2% (computation by horseshoe vortex image method, after Milne-Thompson 1958). With a larger tunnel, with width four times span, the induced power reduction is 5.7%, and so is virtually negligible within likely experimental error. (The correction is critically dependent on tunnel shape: other rectangular shapes may be more favourable.) The corrections are small in the wind tunnel because the vortex wake is essentially parallel to the boundaries of the tunnel, and for large tunnels has little opportunity to interact with those boundaries. In most cases this induced drag correction is independent of speed, provided that speed is not so low that the wing approaches stall and the boundary layer airflows are disturbed. Most workers who have experimented with flying birds in wind tunnels have assumed (usually implicitly) that boundary corrections can be neglected when the tunnel is broader than two or three times the wingspan: this is the usual ‘rule of thumb’ applied for aircraft wing models in wind tunnels. On the basis of the horseshoe vortex or elliptic loading approximations this seems reasonable; if necessary, a simple correction can be determined, although this has rarely been done in such

experiments. Although the corrections to induced power are independent of speed, the corrections to total mechanical power do depend on speed because induced power forms an increasing proportion of total power at lower flight speeds (see, for example, Rayner 1988).

This effect has not normally been considered in calibrating performance measurements in wind tunnels. It is, however, not the sole source of distortion of induced power because of wake–boundary interactions. In relatively slow forward flapping flight of most, if not all, birds and bats the vortex wake comprises a sequence of ring vortices inclined below and behind the animal (Kokshaysky 1979; Kokshaysky & Petrovskii 1979; Rayner 1979*b, c*, 1988; Spedding *et al.* 1984; etc.): the vortices in this wake are not parallel to the tunnel floor, and at some distance downstream of the bird will approach the wall, which can therefore have some effect on induced power. As speed decreases, the inclination of the centre lines of the vortex rings (along which the rings travel) becomes steeper, and the potential for interactions with the tunnel floor, and – by analogy with the situation in hovering – for the development of large-scale ordered vortex structures within the tunnel, becomes greater. The correction to induced power in hovering is large. Thus in flapping flight we may expect the induced drag correction to become larger as flight speed falls.

At forward cruising speeds, induced power is relatively small, and forms typically $\frac{1}{3}$ – $\frac{1}{4}$ of the total mechanical power output (Rayner 1979*c*, 1988). As speed reduces, induced power becomes progressively more important, until in vertebrates it dominates other mechanical energy losses in hovering, and therefore the correction to total power resulting from wall interactions becomes greater. At the same time, our arguments imply that the correction to induced power to account for the boundaries becomes progressively larger still, resulting from changes in the flow pattern around the animal. These effects have yet to be formally quantified but, by inference from our results for hovering flight above, are likely to be significant.

3. EXPERIMENTAL EVIDENCE

Flow visualization observations of the wake of birds flying slowly or hovering within confined spaces typically show a complex chaotic and highly turbulent flow reflecting the interactions of the periodic wake elements with the boundaries (J. M. V. Rayner & A. L. R. Thomas, unpublished observations). Such flows are difficult to interpret, and it rarely proves possible to quantify the wake vortex distributions.

Figure 6 illustrates one observation in which the flow patterns were sufficiently structured to be readily interpreted. The bird is a white-rumped munia (*Lonchura striata*; Passeriformes, Estrildidae), commonly known as a space bird, and is flying very slowly in still air within a large flight tunnel. The working section of the tunnel had wooden or glass walls and square cross-section 1 m in height and width, and was 1.5 m in length, with open ends attached to long, loose fabric

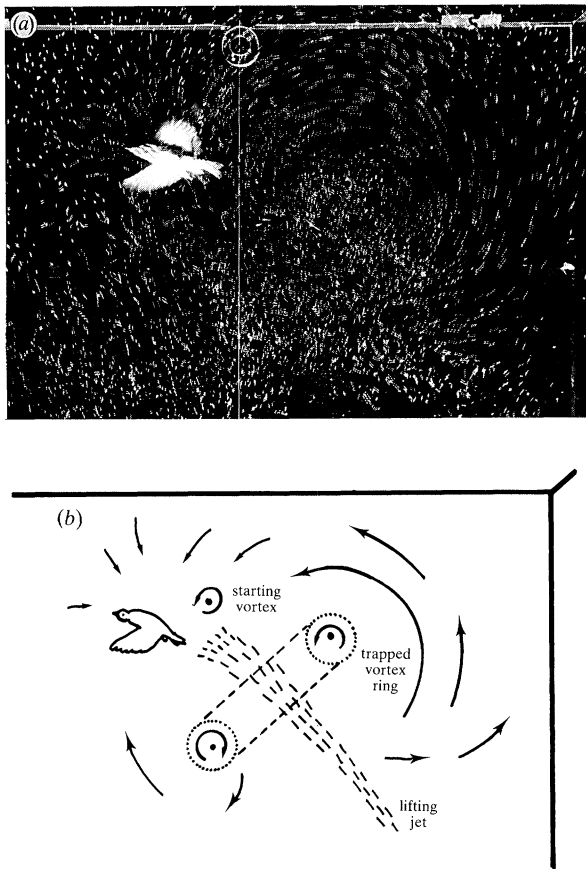


Figure 6. Flow patterns in the wake of a slow-flying finch *Lonchura striata* (flight speed 1 m s^{-1} , mass 14 g, wingspan 16 cm) in a flight tunnel of square cross-section 1 m. (a) photograph of the wake visualized by a cloud of neutrally-buoyant helium-filled soap bubbles; for method see Spedding *et al.* (1984). The top, back right corner of the tunnel is visible. (b) tracing of (a), showing the predominant features: a starting vortex corresponding to the downstroke during which the bird is photographed, a turbulent jet below and behind the bird, and a large vortex ring (axes 50 and 42 cm) axial to and perpendicular to this jet driving an intense recirculation within the flight tunnel. The rightmost side of the ring is more concentrated, and therefore more readily visible, than the leftmost side, which, because of the tilt of the wake and the ring, is closer to the ground plane. This effect is typical both of the individual vortex rings generated in slow flapping flight by birds and bats, and of the larger rings developed in interference flows.

tubes within which the bird could fly freely. The wingspan of the finch was 16 cm, or approximately $\frac{1}{6}$ of the cage cross-section, and its mass was 14 g. Flight speed was approximately 1 m s^{-1} , so that with a wingbeat frequency of $30 \pm 1 \text{ Hz}$ the bird would perform approximately 45 wingbeats while passing through the section. When photographed, the bird was at the mid-point of the section, so there was the opportunity for the vortex rings produced by 15 or 20 wingbeats to have interacted within the floor and sides of the section. The floor was visualized and photographed by the 'helium bubble' method of Spedding *et al.* (1984); figure 6a shows the flow pattern, and figure 6b shows the main features of the flow.

As is typical for small birds of this kind, all aerodynamic lifting force is generated during the

downstroke. The picture includes eight images spaced through a downstroke: the starting vortex for his downstroke is clearly visible. A steeply inclined, narrow turbulent wake below and behind the bird has a mean axial flow speed in the far field of 4.7 m s^{-1} (determined from measurement of the speeds of ten bubbles). This wake is the reaction of the lift forces supporting and propelling the bird. At the resolution of this photograph, the individual vortex elements forming the boundary of the wake are not distinguishable, and the bird is sufficiently small that they may have coalesced (cf. Rayner 1979a). For the ideal momentum jet for this bird in hovering, the induced downwash at the wing disc u_0 is 1.68 m s^{-1} . As the forward speed is 1 m s^{-1} , the angle of the far-field wake to the vertical should be approximately $\tan^{-1}(1/1.68)$, or 31° ; the measured inclination is around 35° , which shows considerable consistency with the prediction, and suggests that the bird is probably flying steadily in force equilibrium. If the far field wake were an ideal momentum jet, the convection velocity u'_1 far below the bird in unconfined hovering should therefore be 3.36 m s^{-1} . The measured value of 4.7 m s^{-1} is somewhat higher than expected for the momentum jet in the far field, and may reflect a change in the nature of this flow. Moreover, the classical momentum jet model is not directly relevant in this situation because the bird is not strictly hovering, and the flow field observed differs from that supposed by the model.

The most striking feature of the flow is the strong recirculation that has developed. This appears to be driven by a small-cored elliptic vortex ring of diameter 50 cm parallel to the axis of the flight tunnel, and 42 cm transverse, oriented at an angle of about $35 \pm 5^\circ$, that is, perpendicular to the axis of the lifting jet. The core radius is approximately 3 cm, but the upstream side of the core is smaller and more obvious than the downstream side below the bird. This ring is situated below and surrounding the bird, yet is approximately three times larger than the wingspan. It cannot have been generated by a single downstroke in the normal way (see, for example, Rayner 1979b; Spedding *et al.* 1984), as such rings cannot exceed the wingspan in diameter, and in fact are often considerably smaller than the wingspan (J. M. V. Rayner & A. L. R. Thomas, unpublished observations). We consider that this ring has been formed by aggregation of some or all of the vorticity generated by a number of downstrokes, and is very closely analogous to the ring that develops beneath a helicopter in the 'vortex ring' state (see above). This implies that the air current in the far field below the bird is not a momentum jet, but has become more diffuse as there may be no thin vortex sheet to provide a discrete boundary. We cannot distinguish a vortex tube forming the boundary of this far-field wake, but the wake is narrow and it is possible that a thin sheet would not be resolved by this flow visualization technique. We suggest tentatively that this change in the jet structure may explain the high velocity measured in the core of this jet.

The large, trapped vortex ring also provides a further explanation for the reduction in downwash at the wing disc, that is, for the positive value of w . The

trapped ring recirculates air downwards past the bird. The bird has to accelerate air to a sufficient extent to support its weight, but some of this downwash is provided by the trapped ring, and the total downwash required ($u_i - w$) is less than that for the unencumbered jet (u_i); therefore w is upwards.

From the gross flow patterns within the tunnel section we may deduce that the airflows created by the slow-flying finch have had an influence on the flow of a much greater volume of air than would normally be supposed, and that this primarily results from interference between vortices in the wake and the side walls and floor of the tunnel. The overall impression of the flow illustrated in figure 6 is very similar to the pattern sketched for a hovering bird in a fully confined volume in figure 1, and this is to be expected as, at this very low flight speed, downwash around the wing disc exceeds forward air speed. It seems reasonable that in a stationary hovering bird a flow of this kind could develop and remain steady: vorticity generated by aerofoil action on the wings at the wing disc is convected downwards and drawn into a large trapped vortex ring below the animal. This concept would appear to imply that the trapped ring should grow indefinitely in strength. However, vorticity of the opposite sense is generated in the boundary layer on the tunnel floor and walls, and this should therefore ensure that the total vorticity within the flow tends to a finite limit. (This conceptual mechanical limit does not necessarily imply that an animal is physiologically capable of sustaining hovering, either within a confined volume or in unconfined air.)

Further experimental evidence from animals of a range of sizes and flight characteristics is essential if we are to quantify the effect of the wake–boundary interactions in hovering or forward flight in confined volumes, and are to justify our claim that they have a substantial effect on airflow within the volume and on induced power. Figure 6 shows that these interactions are particularly large even when the volume dimensions are several times the wingspan, and provides further support to our assertion that even the inviscid theory developed above may in fact overestimate the induced power required to hover in these circumstances.

4. DISCUSSION

This paper has been intended more to recognize an otherwise neglected problem than to provide a formal resolution for it. A detailed quantitative exploration of the implications of our conclusions for extant or future experimental results would therefore be premature and potentially misleading.

Our most significant conclusion is that performance measurements for animals flying slowly or hovering within confined volumes may not be representative of the situation in the wild, in the absence of boundaries. In particular, measured induced power, or total metabolic power, may be significantly lower than the values which apply to unrestrained hovering in an uncluttered space. We would be cautious at this stage

before estimating the magnitude of the errors hidden by such measurements, but they are clearly underestimates, are dependent on the ratio of the dimensions of the bounding volume to the wingspan, and appear to be significant at values of this ratio markedly larger than would be expected from normal wind tunnel forward flight interference corrections. We would not be surprised that, in circumstances when the dimensions of the volume were between two and three times the wingspan, the induced power for hovering was underestimated by as much as 30–50%. This theoretical problem will be resolved only by a more refined theory able to take account of friction on the walls and floor of the bounding volume, and of the presence of large-scale ordered vortex structures superimposed upon the wake vortices generated by the animal's individual wingbeats.

We have argued that in forward flight the correction to total flight power for boundary effects depends also on speed, as a result of the increase in induced power, and the change in wake structure and geometry, of a flying bird as its speed reduces. At lower speeds within a wind tunnel or a solid-walled cage the wake has greater opportunity to interact with the floor, and therefore the potential for induced power to be reduced by interference increases as speed reduces. We are unable to quantify this effect precisely at present. There are many behavioural, physiological and mechanical reasons to expect that flight in a wind tunnel may be distorted by comparison with free flight in the wild. Some, although not all, measurements of total metabolic power in relation to flight speed have given the apparently anomalous result that – within measurement error – power does not vary with speed; certain of these measurements include very slow flight or even hovering (see, for example, Rayner 1988, 1990; Butler & Woakes 1990; Walsberg 1990). This result conflicts with aerodynamic theories which consistently, and apparently inescapably, predict total mechanical power in flight to vary with speed according to a U-shaped curve. Several possible explanations for this discrepancy have been considered, but none so far advanced has carried any great conviction. Aerodynamic artefacts arising from the wind tunnel boundaries have not hitherto been discussed. In this paper we have identified a possible source of bias in the induced power, which is influenced by proximity to the tunnel boundary even when the tunnel is relatively large, and for which the appropriate correction represents a reduction in induced power, and which becomes larger at lower speeds. We conjecture that this may form at least a partial explanation for the otherwise perplexing result that metabolic power is independent of speed. The segments of the measured curves corresponding to flight at faster speeds would be the more typical of free flight, although at lower speeds power for free flight would be underestimated by the wind tunnel measurements. If the degree of this underestimate were comparable to the increase in induced drag resulting from the lower speed, the total power as measured in the wind tunnel could appear to be approximately constant, at least over a range of speeds.

Our work on vertebrate flight aerodynamics has been supported by research grants from the SERC and the Royal Society, and by the award of a Royal Society 1983 University Research Fellowship to J.M.V.R. We are grateful to Professor T. J. Pedley for comments on the manuscript.

REFERENCES

- Aldridge, H. D. J. N. 1988 Flight kinematics and energetics in the little brown bat, *Myotis lucifugus* (Chiroptera: Vespertilionidae), with reference to the influence of ground effect. *J. Zool.* **216**, 507–517.
- Betz, A. 1937 Die Hubschraube in Bodennähe. *Jb. dt. Luftforsch.*, pp. 1238–1240. Translated as *NACA Tech. Mem.* **836**.
- Blake, R. W. 1979 The energetics of hovering in mandarin fish (*Synchropus picturatus*). *J. exp. Biol.* **82**, 25–33.
- Blake, R. W. 1983 Mechanics of gliding in birds with special reference to the influence of ground effect. *J. Biomech.* **16**, 649–654.
- Butler, P. J. & Woakes, A. J. 1990 The physiology of bird flight. In *Bird migration* (ed. E. Gwinner), pp. 300–318. Heidelberg: Springer Verlag.
- Doligalski, T. L. & Walker, J. D. A. 1984 The boundary layer induced by a convected two-dimensional vortex. *J. Fluid Mech.* **139**, 1–28.
- Ellington, C. P. 1984 The aerodynamics of hovering insect flight. Parts I–VI. *Phil. Trans. R. Soc. Lond.* **B305**, 1–181.
- Ersoy, S. & Walker, J. D. A. 1985 Viscous flows induced by counter-rotating vortices. *Physics Fluids* **28**, 2687–2698.
- Glauert, H. 1947 *The elements of aerofoil and airscrew theory*. Cambridge University Press.
- Hainsworth, F. R. 1988 Induced drag savings from ground effect and formation flight in brown pelicans. *J. exp. Biol.* **135**, 431–444.
- Harvey, J. K. & Perry, F. J. 1971 Flowfield produced by trailing vortices in the vicinity of the ground. *AIAA JI* **9**, 1659–1660.
- Johnson, W. 1980 *Helicopter theory*. Princeton University Press.
- Kistyakovskii, A. B. 1967 Glissirovaniye i polyet nad ekranom u zhivotnykh. [Gliding and flight over a surface in animals.] *Vest. Zool.* **2**, 3–8.
- Knight, M. & Hefner, R. A. 1937 Static thrust analysis of the lifting airscrew. *NACA Tech. Note* **626**.
- Knight, M. & Hefner, R. A. 1941 Analysis of ground effect on the lifting airscrew. *NACA Tech. Note* **835**.
- Kokshaysky, N. V. 1979 Tracing the wake of a flying bird. *Nature, Lond.* **279**, 146–148.
- Kokshaysky, N. V. & Pyetrovskii, V. I. 1979 Pryedvarityel'nyiye dannyiye o kharaktyere slyeda za lyetashcheyi ptitsyey. [Preliminary data on the character of the wake of flying birds.] *Dokl. Akad. Nauk SSSR* **244**, 1248–1251. Translated in *Dokl. Biophys.* **244**, 41–43.
- Küchemann, D. 1978 *The aerodynamic design of aircraft*. London: Pergamon Press.
- Laitone, E. V. 1989 Comment on “Drag reduction factor due to ground effect”. *J. Aircraft* **27**, 96.
- Lamb, H. 1932 *Hydrodynamics*, 6th edn. Cambridge University Press.
- Lighthill, M. J. 1979 A simple fluid-flow model of ground effect on hovering. *J. Fluid Mech.* **93**, 781–797.
- Milne-Thompson, L. M. 1958 *Theoretical aerodynamics*. London: Macmillan.
- Pope, A. & Harper, J. J. 1966 *Low-speed wind tunnel testing*. New York: John Wiley.
- Rayner, J. M. V. 1979a A vortex theory of animal flight. Part 1. The vortex wake of a hovering animal. *J. Fluid Mech.* **91**, 697–730.
- Rayner, J. M. V. 1979b A vortex theory of animal flight. Part 2. The forward flight of birds. *J. Fluid Mech.* **91**, 731–763.
- Rayner, J. M. V. 1979c A new approach to animal flight mechanics. *J. exp. Biol.* **80**, 17–54.
- Rayner, J. M. V. 1988 Form and function in avian flight. *Curr. Ornithol.* **5**, 1–77.
- Rayner, J. M. V. 1990 The mechanics of flight and bird migration performance. In *Bird migration* (ed. E. Gwinner), pp. 283–299. Heidelberg: Springer Verlag.
- Rayner, J. M. V. 1991 On the aerodynamics of animal flight in ground effect. *Phil. Trans. R. Soc. Lond.* **B334**, 119–128.
- Reid, E. G. 1932 *Applied wind theory*. New York: McGraw-Hill.
- Shi-Cun, W. 1990 Analytical approach to the induced flow of a helicopter rotor in vertical descent. *J. Am. Helicopter Soc.* **35**, 92–98.
- Spedding, G. R. 1991 The aerodynamics of flight. In *Mechanics of animal locomotion* (ed. R. McN. Alexander). Heidelberg: Springer Verlag. (In the press.)
- Spedding, G. R., Rayner, J. M. V. & Pennycuik, C. J. 1984 Momentum and energy in the wake of a pigeon (*Columba livia*) in slow flight. *J. exp. Biol.* **111**, 81–102.
- Walker, J. D. A., Smith, C. R., Cerra, A. W. & Doligalski, T. L. 1987 The impact of a vortex ring on a wall. *J. Fluid Mech.* **181**, 99–140.
- Walsberg, G. E. 1990 Problems inhibiting energetic analyses of migration. In *Bird migration* (ed. E. Gwinner), pp. 413–421. Heidelberg: Springer Verlag.
- Withers, P. C. & Timko, P. L. 1977 The significance of ground effect to the aerodynamic cost of flight and energetics of the black skimmer (*Rhynchops nigra*). *J. exp. Biol.* **70**, 13–26.
- Zbrozek, J. 1947 Ground effect on the lifting rotor. *A.R.C. Rep. & Mem.* **2347**.

Received 14 March 1991; accepted 27 June 1991

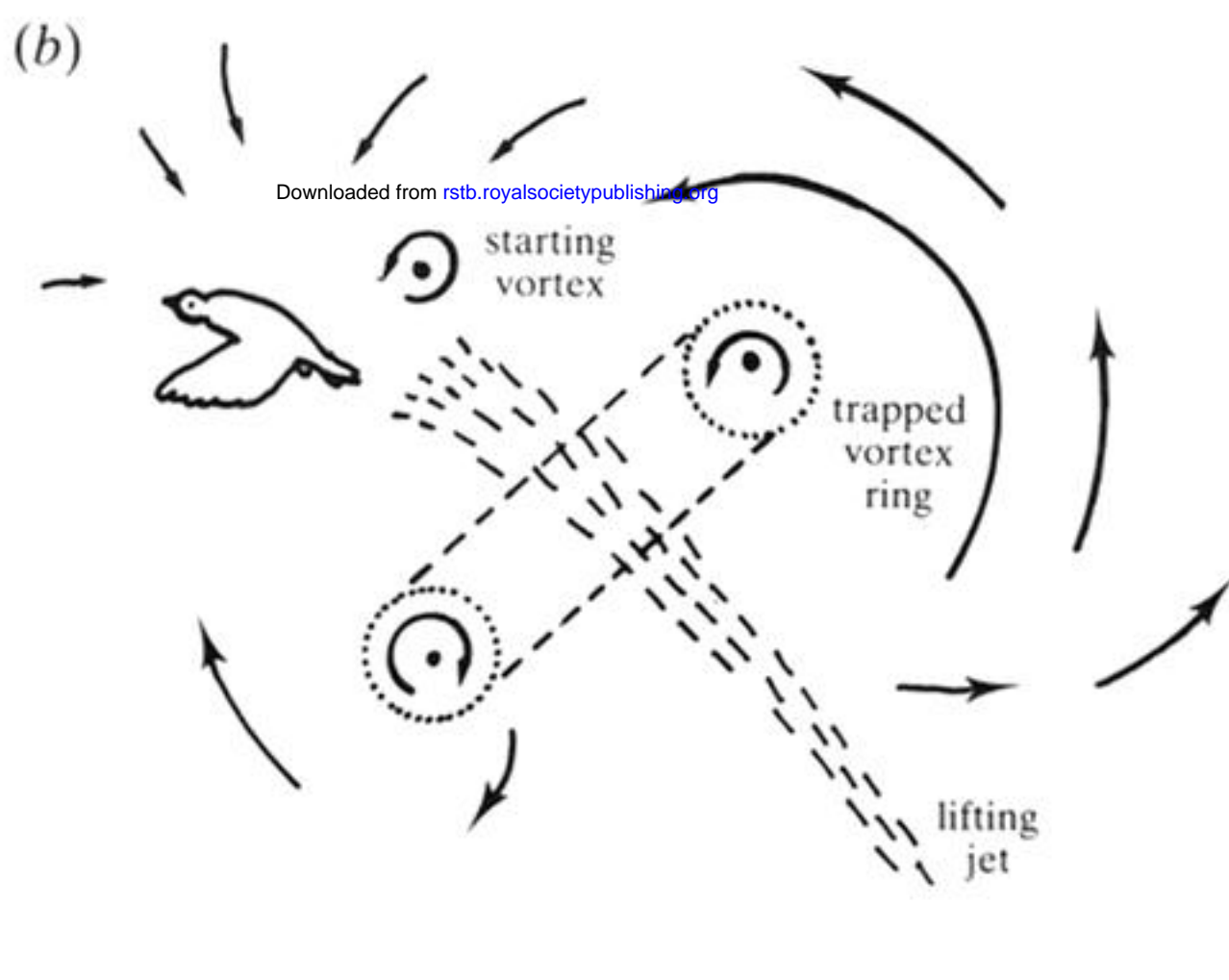
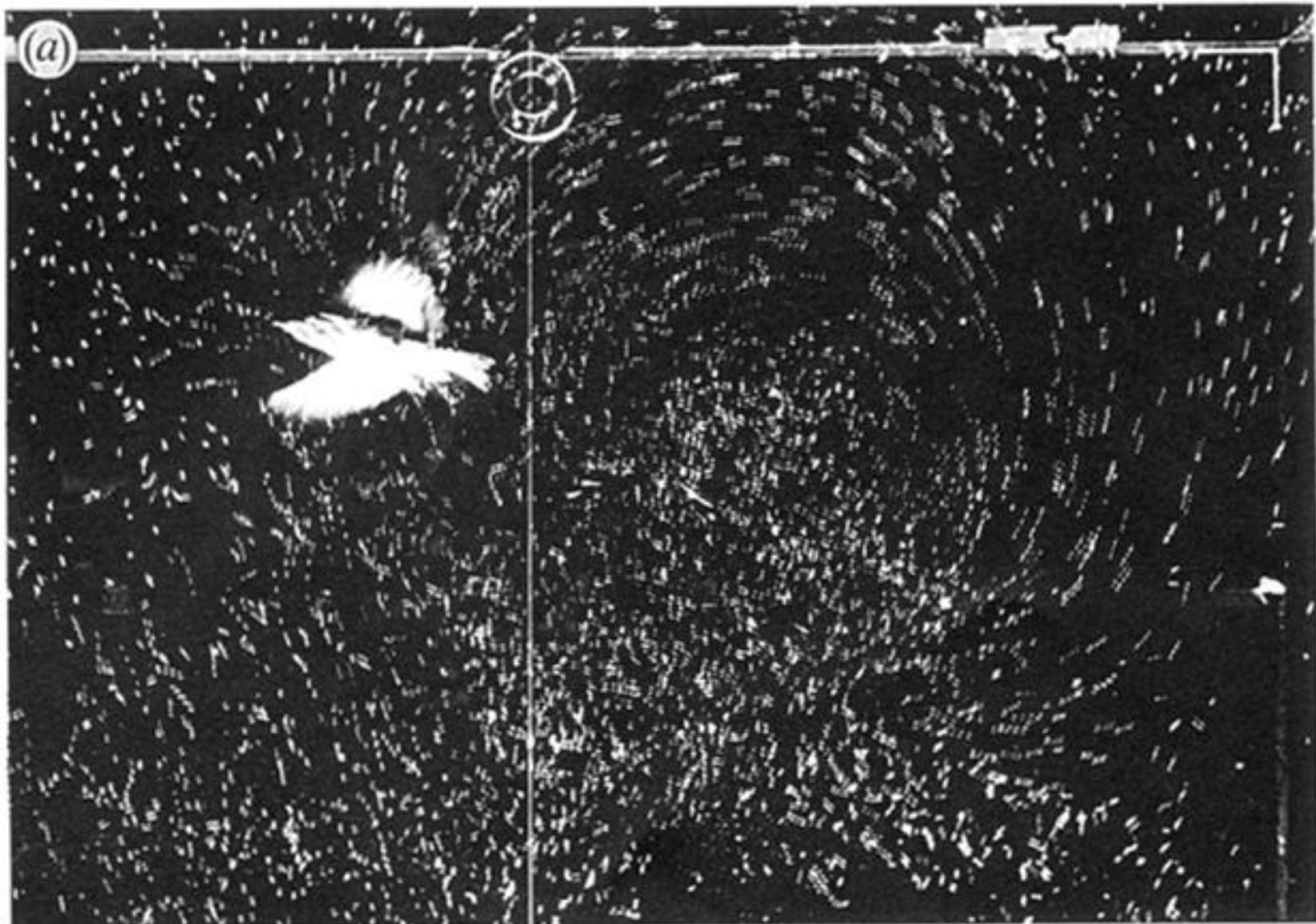


Figure 6. Flow patterns in the wake of a slow-flying finch (*Pinchura striata*) (flight speed 1 m s^{-1} , mass 14 g, wingspan 10 cm) in a flight tunnel of square cross-section 1 m. (a) Photograph of the wake visualized by a cloud of neutrally-buoyant helium-filled soap bubbles; for method see Spedding *et al.* (1984). The top, back right corner of the tunnel is visible. (b) tracing of (a), showing the predominant features: starting vortex corresponding to the downstroke during which the bird is photographed, a turbulent jet below and behind the bird, and a large vortex ring (axes 50 and 42 cm) tilted to and perpendicular to this jet driving an intense circulation within the flight tunnel. The rightmost side of the ring is more concentrated, and therefore more readily visible, than the leftmost side, which, because of the tilt of the wake and the ring, is closer to the ground plane. This effect is typical both of the individual vortex rings generated in slow flapping flight by birds and bats, and of the larger rings developed in interference flows.